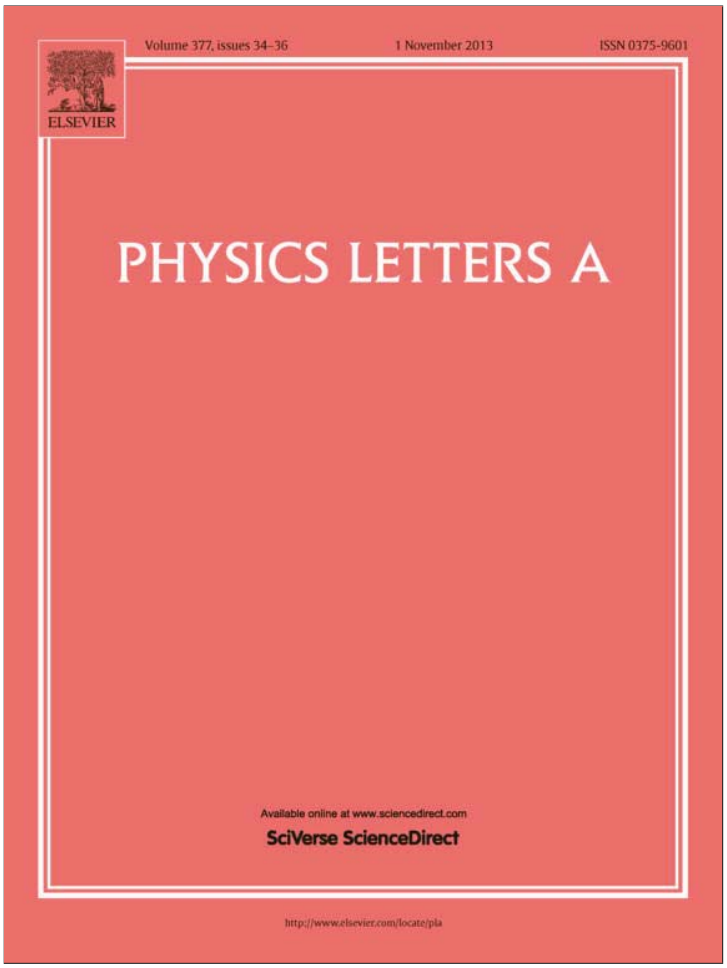

Physics Letters A 377 (2013) 2058–2061

Contents lists available at SciVerse ScienceDirect

Physics Letters A

www.elsevier.com/locate/pla

# Chaotic dynamics of flexible beams with piezoelectric and temperature phenomena

V.A. Krysko [d], J. Awrejcewicz [b,c,*], I.E. Kutepov [d], N.A. Zagniboroda [d], I.V. Papkova [d], A.V. Serebryakov [d], A.V. Krysko [a]

[a] Department of Applied Mathematics and Systems Analysis, Saratov State Technical University, Politehnicheskaya 77, 410054 Saratov, Russian Federation
[b] Lodz University of Technology, Department of Automation and Biomechanics, 1/15 Stefanowski St., 90-924 Lodz, Poland
[c] Warsaw University of Technology, Department of Vehicles, 84 Narbutta St., 02-524 Warsaw, Poland
[d] Department of Mathematics and Modeling, Saratov State Technical University, Politehnicheskaya 77, 410054 Saratov, Russian Federation

ARTICLE INFO

*Article history:*
Received 13 May 2013
Accepted 25 June 2013
Available online 1 July 2013
Communicated by A.R. Bishop

*Keywords:*
Chaos
Weak turbulence
Beam
Wavelets

ABSTRACT

The Euler–Bernoulli kinematic model as well as the von Kármán geometric non-linearity are used to derive the PDEs governing flexible beam vibrations. The beam is embedded into a 2D temperature field, and its surface is subjected to action of the electric potential. We report how an increase of the exciting load amplitude yields the beam turbulent behavior, and how the temperature changes a scenario from a regular/laminar to spatio-temporal/turbulent dynamics. Both classical Fourier analysis and Morlet wavelets are used to monitor a strong influence of temperature on regular and chaotic beam dynamics.



## 1. Introduction

Recently an attempt to study wave turbulence exhibited by thin elastic plates within "turbulence theories" has been observed. Since wave (weak) turbulence is less mathematically sophisticated than the classical (hydrodynamic) turbulence (see [1,2]) it is tempting to validate feasibility of vibrations of the two-dimensional solids with respect to the existing theoretical models for turbulence.

A series of recently published reports are devoted to an experimental study of the turbulent behavior of a plate within the Föppl–von Kármán model [3–5]. Despite a qualitative good agreement with the kinetic weak turbulence theory, the obtained energy spectrum has not been confirmed by a theoretical prediction. Mordant [6] applied an experimental method for monitoring of both temporal and spatial evolution of wave turbulence exhibited by a thin elastic plate. Various Fourier spectra of the wave deformations were analyzed. Elastic wave turbulence was also reported experimentally while analyzing thin elastic plates [7]. It was shown that when the total energies in wave fields were small, the obtained energy spectra fitted well with a statically steady solution of the weak kinetic turbulence theory.

Other researchers focused only on the theoretical and numerical simulation studying 2D structural members (mainly flexible plates). Touzé et al. used the von Kármán PDEs to study both experimentally and numerically a scenario of transition to wave turbulence exhibited by thin vibrating plates. Large amplitude plate vibrations were monitored while analyzing two bifurcations which separated three distinct regimes: periodic, quasi-periodic and spatio-temporal chaos. It is claimed that the third regime (turbulent) is characterized by a broad band Fourier spectrum and an energy cascade from large to small wavelength [8].

It should be emphasized that transition from regular to chaotic dynamics in circular cylindrical shells and doubly-curved panels was numerically reported by Amabili et al. [9–11]. Chaotic vibrations of shallow shell/panel with and without concentrated mass were studied both analytically and experimentally by Nagai et al. [12,13] and Maruyama et al. [14]. Recently, Touzé et al. [15] described a transition to chaotic vibrations for harmonically forced perfect and imperfect circular plates.

This report extends a series of our papers [16–23] devoted to the study of transition from regular (periodic and quasi-periodic) vibrations to chaotic ones in continuous mechanical systems (plates, cylindrical shells, panels and sector-type spherical shells).

In this Letter, however, we address the problem related to large deflations of beams, plates and shells, when the structural members are subjected to the action of temperature field and piezoelectric phenomena [24].

* Corresponding author at: Lodz University of Technology, Department of Automation and Biomechanics, 1/15 Stefanowski St., 90-924 Lodz, Poland.
*E-mail address:* awrejcew@p.lodz.pl (J. Awrejcewicz).

0375-9601/$ – see front matter 
http://dx.doi.org/10.1016/j.physleta.2013.06.040

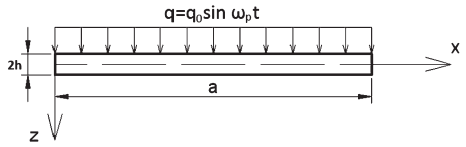


**Fig. 1.** Scheme of the analyzed beam.

## 2. Mathematical model

We apply the following assumption to derive the governing equations: (1) the Euler–Bernoulli kinematic model is used; (2) 2D temperature field model is applied; (3) beam surface is subjected to the action of the electric potential difference $V(t)$ – boundary of the studied space is not covered by the electrodes; (4) geometric non-linearity is taken in the von Kármán form – see Fig. 1.

Stress-strain equations including linear formulas for direct and inverse piezoelectric and pyroelectric effects are given in the following form:

$$\sigma_{xx} = c_{11}^E(\varepsilon_{xx} - \alpha_T T) - e_{31}E_z, \qquad D_x = \varepsilon_{11}^S E_x,$$
$$D_z = \varepsilon_{33}^S E_z + e_{31}\varepsilon_{xx} + g_{pyr}T. \tag{1}$$

We use the following physical constants for the material: $c_{11}^E$ – elasticity modulus (for constant electric field); $e_{31}$ – piezoelectric coefficient; $\varepsilon_{11}^S, \varepsilon_{33}^S$ – dielectric permittivity (for constant deformation); $\alpha_T$ – linear heat extension coefficient; $T = \theta(x,z,t) - T_0$ – temperature increase with respect to the initial temperature $T_0$; $g_{pyr}$ – pyroelectric coefficient; $g_{pyr} = (2\ldots3)\cdot 10^{-3}$ C/(m K) in the direction of initial polarization, and $g_{pyr} = 0$ for remaining directions. State equations (1) refer to the situation when the beam material has already been polarized with respect to the beam thickness. Vector characteristics of the electric field are as follows: $\mathbf{D} = \mathbf{D}(x,z,t)$ – induction, $\mathbf{E} = \mathbf{E}(x,z,t)$ – intensity.

Applying the variation relations the following equations are derived:

$$k_1^2\frac{\partial^2 w}{\partial x^2} + \frac{1}{\lambda^2}\frac{\varepsilon_{11}^S}{\varepsilon_{33}^S}\frac{\partial^2\psi}{\partial x^2} + \frac{\partial^2\psi}{\partial z^2} - k_{pyr}^2\lambda^2\frac{\partial T}{\partial z} = 0, \tag{2}$$

$$\frac{\partial^2 u}{\partial x^2} + L_3(w,w) - \lambda^2(\alpha_T T_0)\int_{-1/2}^{1/2}\frac{\partial T}{\partial x}\,dz = \ddot{u} + \varepsilon_1\dot{u}, \tag{3}$$

$$\frac{1}{\lambda^2}\left(L_1(u,w) + L_2(w,w) - \frac{1}{12}\frac{\partial^4 w}{\partial x^4} + q + k_2^2\cdot V(t)\cdot\frac{\partial^2 w}{\partial x^2}\right) - (\alpha_T T_0)\times\left(\int_{-1/2}^{1/2}\frac{\partial^2 T}{\partial x^2}z\,dz + \frac{\partial^2 w}{\partial x^2}\int_{-1/2}^{1/2}T\,dz + \frac{\partial w}{\partial x}\int_{-1/2}^{1/2}\frac{\partial T}{\partial x}\,dz\right) = \ddot{w} + \varepsilon_2\dot{w}, \tag{4}$$

$$\frac{\partial^2 T}{\partial x^2} + \lambda^2\frac{\partial^2 T}{\partial z^2} = \left[\frac{\rho c_\varepsilon a}{\lambda_q}\sqrt{\frac{c_{11}^E}{\rho}}\right]\frac{\partial T}{\partial t} + \left[\alpha_T a\frac{c_{11}^E + c_{12}^E + c_{13}^E}{\lambda_q}\sqrt{\frac{c_{11}^E}{\rho}}\right]\times\left(\frac{\partial\dot{u}}{\partial x} + \frac{1}{\lambda^2}\frac{\partial w}{\partial x}\frac{\partial\dot{w}}{\partial x} - \frac{1}{\lambda^2}z\frac{\partial^2\dot{w}}{\partial x^2}\right) - \left[\frac{a}{\lambda_q}\frac{g_{pyr}}{d_{31}}\sqrt{\frac{c_{11}^E}{\rho}}\right]\times\frac{1}{\lambda^2}\frac{\partial\dot{\psi}}{\partial z}, \tag{5}$$

where: $L_1(u,w) = \frac{\partial u}{\partial x}\frac{\partial^2 w}{\partial x^2} + \frac{\partial^2 u}{\partial x^2}\frac{\partial w}{\partial x}$, $L_2(w,w) = \frac{3}{2}\frac{\partial^2 w}{\partial x^2}(\frac{\partial w}{\partial x})^2$, $L_3(w,w) = \frac{\partial w}{\partial x}\frac{\partial^2 w}{\partial x^2} = \frac{1}{2}L_1(w,w)$, and the electric potential $\psi = \psi(x,z,t)$ satisfies the following electrostatic equations $\frac{\partial D_x}{\partial x} + \frac{\partial D_z}{\partial z} = 0$, $E_x = -\frac{\partial\psi}{\partial x}$, $E_z = -\frac{\partial\psi}{\partial z}$. Eqs. (2)–(5) are associated with the following boundary conditions for the electric potential:

$$\psi(x,-1/2,t) = -V(t)/2,$$
$$\psi(x,1/2,t) = V(t)/2 \quad (0\leqslant x\leqslant 1, t>0), \tag{6}$$
$$\frac{\partial\psi}{\partial x} = 0. \tag{7}$$

For the functions characterizing the stress beam state regarding $u(x,t)$, $w(x,t)$ we have,

$$w(0,t) = w(1,t) = u(0,t) = u(1,t) = w_x'(1,t) = 0,$$
$$M_x(0,t) = 0, \tag{8}$$

and in the case of temperature field the first order boundary conditions are applied.

**Table 1**
Vibration charts.

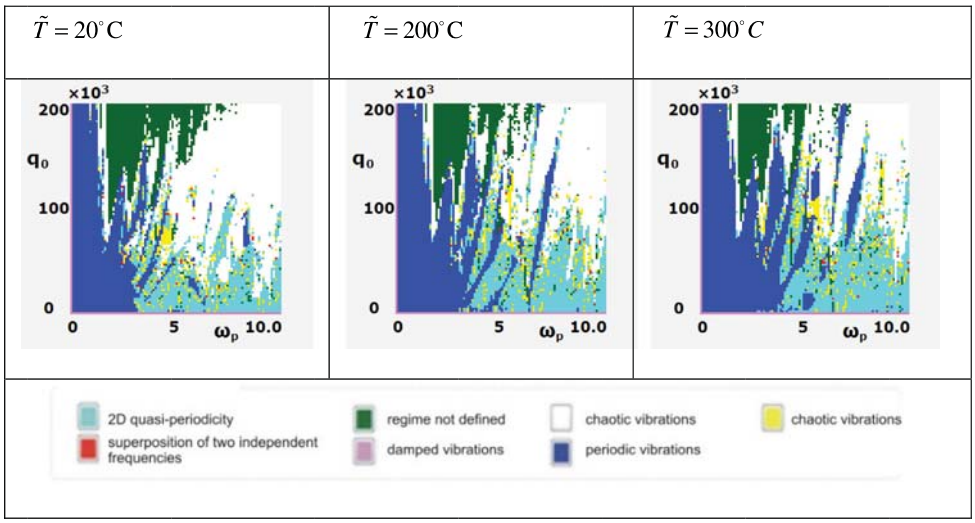

Initial conditions are as follows:

$$\psi(x,z,0)=0,$$
$$\frac{\partial\psi(x,z,0)}{\partial t}=0 \quad (0\leqslant x\leqslant 1,\ -1/2\leqslant z\leqslant 1/2),$$
$$w(x,0)=\dot{w}(x,0)=u(x,0)=\dot{u}(x,0),$$
$$T(x,z,0)=0. \tag{9}$$

System of Eqs. (2)–(9) is transformed to their non-dimensional form in the following way (dimensional quantities are denoted by wave superscript): $c=\sqrt{c_{11}^E/\rho}$ – velocity, $d_{31}$ – piezo-module, $\tilde{x}=a\cdot x$, $\tilde{z}=2h\cdot z$, $\tilde{u}=\frac{(2h)^2}{a}\cdot u$, $\tilde{w}=2h\cdot w$, $\lambda=a/(2h)$, $\tilde{t}=\frac{a}{c}\cdot t$, $\tilde{\varepsilon}_{1,2}=\frac{c}{a}\cdot\varepsilon_{1,2}$, $\tilde{q}=c_{11}^E(\frac{2h}{a})^4\cdot q$, $\tilde{V}=\frac{1}{\lambda^2}(\frac{2h}{d_{31}})\cdot V$, $\tilde{\psi}=\frac{1}{\lambda^2}(\frac{2h}{d_{31}})\cdot\psi$, $\tilde{T}=T_0\cdot T$. In Eqs. (2)–(5) we have $k_1^2=e_{31}d_{31}/\varepsilon_{33}^S$ and $k_2^2=e_{31}/(c_{11}^E d_{31})$ – non-dimensional coefficients of the electro-chemical couplings, and $k_{pyr}^2=g_{pyr}T_0 d_{31}/\varepsilon_{33}^S$ – non-dimensional coefficient of the pyroelectric coupling. Furthermore, $\lambda_q$, $c_\varepsilon$ denote heat transfer coefficient and heat capacity, respectively. In Eq. (5) each of the used brackets represents a non-dimensional term.

## 3. Numerical simulations

As an example, we consider non-linear dynamics of the elastic beam embedded into a stationary temperature field with the electric potential. In this case system (2)–(5) is decoupled into separated solutions, i.e. that of 2D stationary heat transfer equation and into the system (3)–(4). The 2D heat transfer equation for the rectangular area $z\in[-1/2,1/2]$, $x\in[0,1]$ (Fig. 1) is solved via the method of boundary elements, whereas for the beam the problem is reduced to the Cauchy task through the FDM (Finite Difference Method) of the second-order accuracy, and then it is solved via the fourth Runge–Kutta method. As a result, when applying the FDM we introduce the partition into $n=80$ parts of the interval $x\in[0,1]$ and time step $\Delta t=1/256$. We analyzed a set of solutions in the plane of control parameters $\{\omega_p,q_0\}$. The obtained computational results allowed us to construct the following charts. Plane $\{\omega_p,q_0\}$ is divided into $\{100,100\}$ parts, i.e. we need to solve $3\times 10^4$ problems and for each of them we analyze time histories, phase and modal portraits, Poincaré cross-sections and maps, phase and modal portraits, autocorrelation functions, Fourier and Morlet power spectra (Table 1).

One may conclude that the temperature increase causes that the regions of chaotic/turbulent beam dynamics shrink.

Table 2 gives a few studied characteristics (Fourier power spectrum and spatio-temporal chaos) for certain values of $q_0$ and temperature for $\omega_p=5$. The illustrated results exhibit their essential dependence on the temperature.

First two rows of this table ($q_0=35\times 10^3$) show four direct frequency peaks being in agreement with the Morlet power spectrum ($\tilde{T}=20\,^\circ$C). An increase of temperature ($\tilde{T}=200\,^\circ$C) damps the amplitude of two centrally situated frequencies but a series of frequencies with small amplitudes appear instead.

An increase of $q_0$ up to $q_0=95\times 10^3$ exhibits beams turbulent behavior which is manifested by broad-band Fourier and Morlet spectra ($\tilde{T}=20\,^\circ$C). The increase of temperature implies a route of continuous (broad-band) frequency spectrum to that with only two clearly distinguished peaks ($\tilde{T}=300\,^\circ$C). Again, remarkable agreement between the Fourier and Morlet power spectra is manifested.

However, the third computational example ($q_0=135\times 10^3$) cancels a tempting description of the expected dynamics beam behavior as it has been illustrated so far. Namely, for $\tilde{T}=20\,^\circ$C the beam exhibits turbulent dynamics (spatio-temporal chaos), which then transits into regular (quasi-periodic) beam dynamics ($\tilde{T}=200\,^\circ$C) with four distinct frequencies, and then each of them (in spite of excitation frequency) increases its amplitude and generates a series of frequencies via the period doubling bifurcation ($\tilde{T}=300\,^\circ$C) implying a weakly developed turbulent regime.

**Table 2**
Fourier and Morlet power spectra.

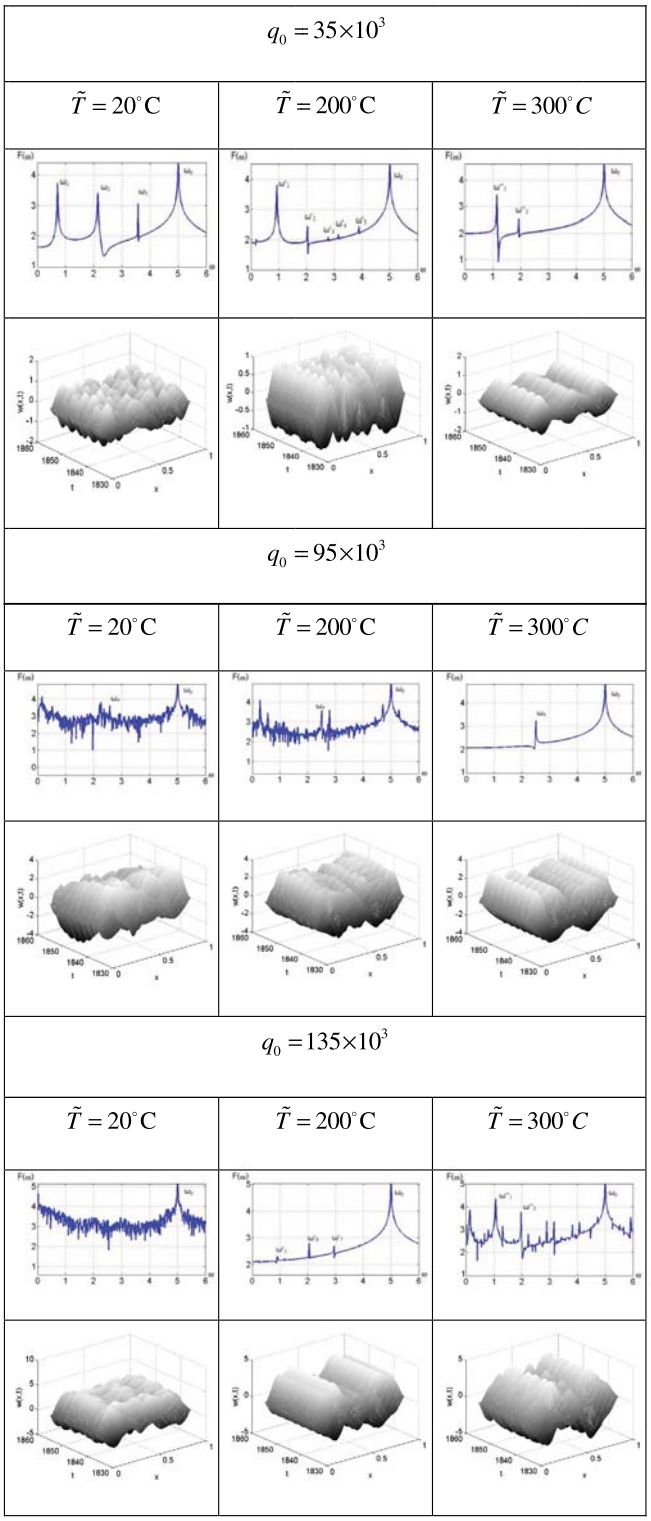


## 4. Conclusions

Regular (periodic and quasi-periodic) and chaotic vibrations of flexible beams taking into account the thermal and piezoelectric

phenomena were described using numerical simulations. In particular, the analysis carried out with the help of the classical Fourier method and the Morlet wavelets implies a strong influence of temperature on both regular and chaotic beam dynamics.

## Acknowledgements

This work was supported by the National Center of Science under the grant MAESTRO 2, No. 2012/04/A/ST8/00738 for the years 2012–2015 (Poland).

## References

[1] V.E. Zakharov, V.S. Lvov, G. Falkovisch, Kolmogorov Spectra of Turbulence I: Wave Turbulence, Springer-Verlag, Berlin, 1992.
[2] U. Frisch, Turbulence, Cambridge University Press, Cambridge, England, 1995.
[3] C. Connaughton, Physica D 238 (2009) 2282.
[4] A. Boudaut, O. Cadot, B. Odille, C. Touzé, Phys. Rev. Lett. 100 (2008) 234504.
[5] N. Mordant, Phys. Rev. Lett. 100 (2008) 124505.
[6] N. Mordant, Eur. Phys. J. B 76 (2010) 537.
[7] N. Yokoyama, M. Takaoka, Phys. Rev. Lett. 110 (2013) 105501.
[8] C. Touzé, S. Bilbao, O. Cadot, J. Sound Vib. 331 (2) (2012) 412.
[9] M. Amabili, A. Sarkar, M.P. Païdoussis, J. Sound Vib. 290 (3–5) (2006) 736.
[10] M. Amabili, Int. J. Non-Linear Mech. 40 (5) (2005) 683.
[11] F. Pellicano, M. Amabili, J. Sound Vib. 93 (1–2) (2006) 227.
[12] K. Nagai S, Maruyama, M. Oya, T. Yamaguchi, Comput. Struct. 82 (2004) 2607.
[13] K. Nagai, S. Maruyama, T. Murata, T. Yamaguchi, J. Sound Vib. 305 (3) (2007) 492.
[14] S. Maruyama, K. Nagai, Y. Tsuruta, J. Sound Vib. 315 (3) (2008) 607.
[15] C. Touzé, O. Thomas, M. Amabili, Int. J. Non-Linear Mech. 46 (1) (2011) 234.
[16] J. Awrejcewicz, V.A. Krysko, A.V. Krysko, Int. J. Bifur. Chaos 12 (7) (2002) 1465.
[17] J. Awrejcewicz, V.A. Krysko, G.G. Narkaitis, Nonlinear Dynam. 32 (2003) 187.
[18] J. Awrejcewicz, V.A. Krysko, N.E. Saveleva, J. Comput. Nonlinear Dyn. 2 (1) (2007) 1.
[19] A.V. Krysko, J. Awrejcewicz, I.V. Papkova, J. Comput. Nonlinear Dyn. 3 (4) (2008) 041006.
[20] J. Awrejcewicz, O.A. Saltykova, M.V. Zhigalov, P. Hagedorn, V.A. Krysko, Int. J. Aerosp. Lightweight Struct. 1 (2) (2011) 203.
[21] J. Awrejcewicz, A.V. Krysko, I.V. Papkova, V.A. Krysko, Chaos Solitons Fractals 45 (2012) 687.
[22] J. Awrejcewicz, A.V. Krysko, I.V. Papkova, V.A. Krysko, Chaos Solitons Fractals 45 (2012) 709.
[23] J. Awrejcewicz, A.V. Krysko, I.V. Papkova, V.A. Krysko, Chaos Solitons Fractals 45 (2012) 721.
[24] J. Awrejcewicz, V.A. Krysko, A.V. Krysko, Thermo-Dynamics of Plates and Shells, Springer-Verlag, New York, 2007.